AMERICAN SOCIETY FOR MICROBIOLOGY | Journal of Virology®

Deficiency of the NOD-Like Receptor NLRC5 Results in Decreased CD8$^+$ T Cell Function and Impaired Viral Clearance

Christopher R. Lupfer,* Kate L. Stokes,* Teneema Kuriakose, Thirumala-Devi Kanneganti

Department of Immunology, St. Jude Children's Research Hospital, Memphis, Tennessee, USA

ABSTRACT Pathogen recognition receptors are vital components of the immune system. Engagement of these receptors is important not only for instigation of innate immune responses to invading pathogens but also for initiating the adaptive immune response. Members of the NOD-like receptor (NLR) family of pathogen recognition receptors have important roles in orchestrating this response. The NLR family member NLRC5 regulates major histocompatibility complex class I (MHC-I) expression during various types of infections, but its role in immunity to influenza A virus (IAV) is not well studied. Here we show that *Nlrc5*$^{-/-}$ mice exhibit an altered CD8$^+$ T cell response during IAV infection compared to that of wild-type (WT) mice. *Nlrc5*$^{-/-}$ mice have decreased MHC-I expression on hematopoietic cells and fewer CD8$^+$ T cells prior to infection. NLRC5 deficiency does not affect the generation of antigen-specific CD8$^+$ T cells following IAV infection; however, a change in epitope dominance is observed in *Nlrc5*$^{-/-}$ mice. Moreover, IAV-specific CD8$^+$ T cells from *Nlrc5*$^{-/-}$ mice have impaired effector functions. This change in the adaptive immune response is associated with impaired viral clearance in *Nlrc5*$^{-/-}$ mice. Collectively, our results demonstrate an important role for NLRC5 in regulation of antiviral immune responses and viral clearance during IAV infection.

IMPORTANCE The NOD-like receptor family member NLRC5 is known to regulate expression of MHC-I as well as other genes required for antigen processing. In addition, NLRC5 also regulates various immune signaling pathways. In this study, we investigated the role of NLRC5 during influenza virus infection and found a major role for NLRC5 in restricting virus replication and promoting viral clearance. The observed increases in viral titers in NLRC5-deficient mice correlated with impaired effector CD8$^+$ T cell responses. Although NLRC5-deficient mice were defective at clearing the virus, they did not show an increase in morbidity or mortality following influenza virus infection because of other compensatory immune mechanisms. Therefore, our study highlights how NLRC5 regulates multiple immune effector mechanisms to promote the host defense during influenza virus infection.

KEYWORDS Nod-like receptor, NLR, NLRC5, influenza A virus, lung, T cell, major histocompatibility complex, MHC, natural killer cell

Influenza A virus (IAV) epidemics are an important cause of morbidity and mortality around the world, resulting in 3 to 5 million severe cases and 250,000 to 500,000 deaths per year (1). The ability of IAV to undergo frequent genetic mutations increases the potential for further epidemics. Therefore, understanding the immune response to IAV is necessary for developing improved therapies and vaccines. The NOD-like receptor (NLR) family is an important group of regulators of both the innate and adaptive immune systems. Multiple NLR family members play essential roles during IAV infection. NLRP3 functions in innate immunity and healing responses during IAV infection (2,

Received 14 March 2017 **Accepted** 5 June 2017

Accepted manuscript posted online 14 June 2017

Citation Lupfer CR, Stokes KL, Kuriakose T, Kanneganti T-D. 2017. Deficiency of the NOD-like receptor NLRC5 results in decreased CD8$^+$ T cell function and impaired viral clearance. J Virol 91:e00377-17. https://doi.org/10.1128/JVI.00377-17.

Editor Rozanne M. Sandri-Goldin, University of California, Irvine

Address correspondence to Thirumala-Devi Kanneganti, Thirumala-Devi.Kanneganti@StJude.org.

* Present address: Christopher R. Lupfer, Department of Biology, Missouri State University, Springfield, Missouri, USA; Kate L. Stokes, Department of Cancer Biology, Abramson Family Cancer Research Institute, and Perelman School of Medicine at the University of Pennsylvania, Philadelphia, Pennsylvania, USA.

C.R.L. and K.L.S. contributed equally to this article.

3) as well as in adaptive immune responses (4). Furthermore, NOD2-deficient mice exhibit decreased type I interferon (IFN) production (5) and diminished $CD8^+$ T cell generation in response to IAV (6).

Though traditionally thought of as immune sensors, NLRs also participate in the modulation of immune signaling pathways and functions. Class II transactivator (CIITA), a member of the NLR family, regulates the transcription of major histocompatibility complex class II (MHC-II) genes (7). NLRC5 comparably regulates the expression of major histocompatibility complex class I (MHC-I) genes (8). In addition, NLRC5 regulates the expression of genes required for antigen processing, such as the β2-microglobulin, Tap1, and Lmp2 genes (8–10). NLRC5 is expressed in most hematopoietic cells, including myeloid cells, $CD4^+$ and $CD8^+$ T cells, B cells, natural killer (NK) cells, and natural killer T (NKT) cells (9, 11). However, the breadth of function of NLRC5 during infection has not been examined fully.

Various studies have reported contradictory roles for NLRC5 in other immune signaling pathways. *In vitro* overexpression or small interfering RNA (siRNA)-mediated knockdown of NLRC5 suggested roles for NLRC5 as an inhibitor of NF-κB signaling (12, 13) and an activator of type I IFN production (14, 15). However, infections with viruses or bacteria in knockout mice or cells derived from knockout mice did not duplicate these results, and no differences in NF-κB-dependent gene expression were observed (16, 17). IFN-γ and $CD8^+$ T cell levels, however, have been shown to decrease in *Nlrc5*$^{-/-}$ mice compared to those in wild-type (WT) mice during *Listeria monocytogenes* infection (10, 16).

Here we report on a previously unexplored role for NLRC5 during IAV infection *in vivo*. Our results show that *Nlrc5*$^{-/-}$ mice have an intrinsic defect in MHC-I expression on a variety of cell types. Moreover, a reduction in the total number of $CD8^+$ T cells is also observed in *Nlrc5*$^{-/-}$ mice prior to infection. Notably, NLRC5 deficiency leads to impaired $CD8^+$ T cell effector functions and delayed viral clearance during IAV infection. Together, our data identify NLRC5 as a modulator of $CD8^+$ T cell responses during IAV infection.

RESULTS

***In vitro* functions of NLRC5.** In addition to its role as a regulator of MHC-I expression (8), multiple studies have linked NLRC5 to control of the NF-κB pathway or regulation of type I interferon (IFN) production. However, there have been conflicting reports of NLRC5 either potentiating (14, 15, 18), suppressing (12, 13, 19), or having no effect on (16, 17) NF-κB or IFN production. It has further been reported that NLRC5 may function during activation of the inflammasome (16, 20, 21). Therefore, to address the role of NLRC5 during IAV infection, we infected WT or *Nlrc5*$^{-/-}$ bone marrow-derived dendritic cells (BMDCs) with the influenza A/Puerto Rico/8/34 H1N1 virus (PR8) or the influenza A/HKx31 H3N2 virus (x31). We did not detect any defect in the activation of caspase-1 or the production of interleukin-1β (IL-1β) *in vitro* following infection with either virus (Fig. 1A and B and 2A and B). Type I IFN responses during infection with PR8 tended to be higher in *Nlrc5*$^{-/-}$ BMDCs (Fig. 1C), and infection with x31 induced significantly higher levels of *Ifnb* in *Nlrc5*$^{-/-}$ BMDCs than in WT cells (Fig. 2C). Regardless of the virus, we consistently observed increased activation of the mitogen-activated protein (MAP) kinase extracellular signal-regulated kinase (ERK) and of NF-κB as well as increased production of the NF-κB-dependent cytokine IL-6 in *Nlrc5*$^{-/-}$ BMDCs compared to that in WT cells (Fig. 1D and E and 2D and E). We also examined the expression of MHC-I on BMDCs before and after infection with IAV. Similar to previous reports, the absence of NLRC5 was associated with decreased expression of both H2-D^b and H2-K^b MHC-I molecules (Fig. 1F and G and 2F and G).

***Nlrc5*-deficient mice have reduced MHC-I expression *in vivo*.** The differences in NF-κB activation and MHC-I expression *in vitro* prompted us to examine the role of NLRC5 during PR8 infection *in vivo*. To this end, we infected WT and *Nlrc5*$^{-/-}$ mice intranasally (i.n.) with 900 PFU of PR8. Unlike our *in vitro* results, we found no differences in the amounts of either IL-6 or IL-1β in the lungs of *Nlrc5*$^{-/-}$ mice and WT

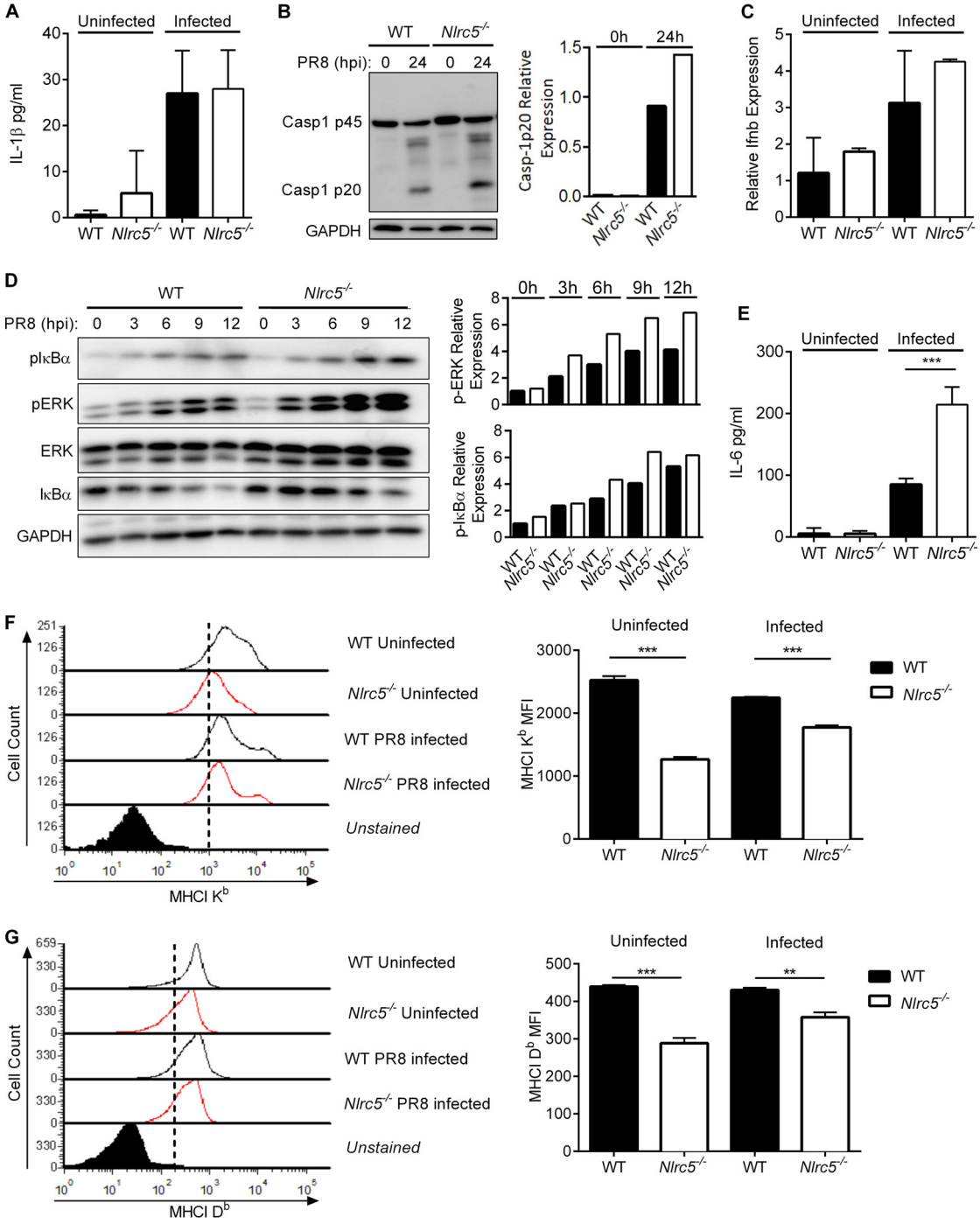

FIG 1 NLRC5 control of immune pathways during PR8 infection *in vitro*. BMDCs from WT and *Nlrc5*$^{-/-}$ mice were mock infected or infected at an MOI of 10 with influenza A/PR/8/34 H1N1 (PR8) virus for 24 h. (A) IL-1β levels in culture supernatants of uninfected and PR8-infected BMDCs. (B) Western blotting of WT and *Nlrc5*$^{-/-}$ BMDC lysates for pro-caspase-1 (p45) and active caspase-1 (p20). (C) Expression levels of IFN-β (*Ifnb*) relative to those of β-actin in uninfected and PR8-infected BMDCs. (D) WT and *Nlrc5*$^{-/-}$ BMDC lysates collected at the indicated time points were analyzed by Western blotting for phosphorylated and total ERK MAP kinase and IκBα as well as a glyceraldehyde-3-phosphate dehydrogenase (GAPDH) loading control. (E) IL-6 levels in the culture supernatants of uninfected or PR8-infected BMDCs. (F and G) MHC-I K^b and D^b isoform expression levels were measured by flow cytometry and presented as geometric mean fluorescence intensities (MFI). Data are representative of two or three independent experiments (n = 2 or 3 wells per experiment) and are means ± SEM. **, $P < 0.01$; ***, $P < 0.001$ (two-sided unpaired Student's t test).

controls (Fig. 3A and B). We further examined leukocyte infiltration into the lungs but found no differences in neutrophil numbers between WT and *Nlrc5*$^{-/-}$ mice (Fig. 3C). Consistent with our *in vitro* data, the expression of MHC-I H2-K^b and H2-D^b was significantly lower on lymphocytes isolated from the lungs of *Nlrc5*$^{-/-}$ mice than on

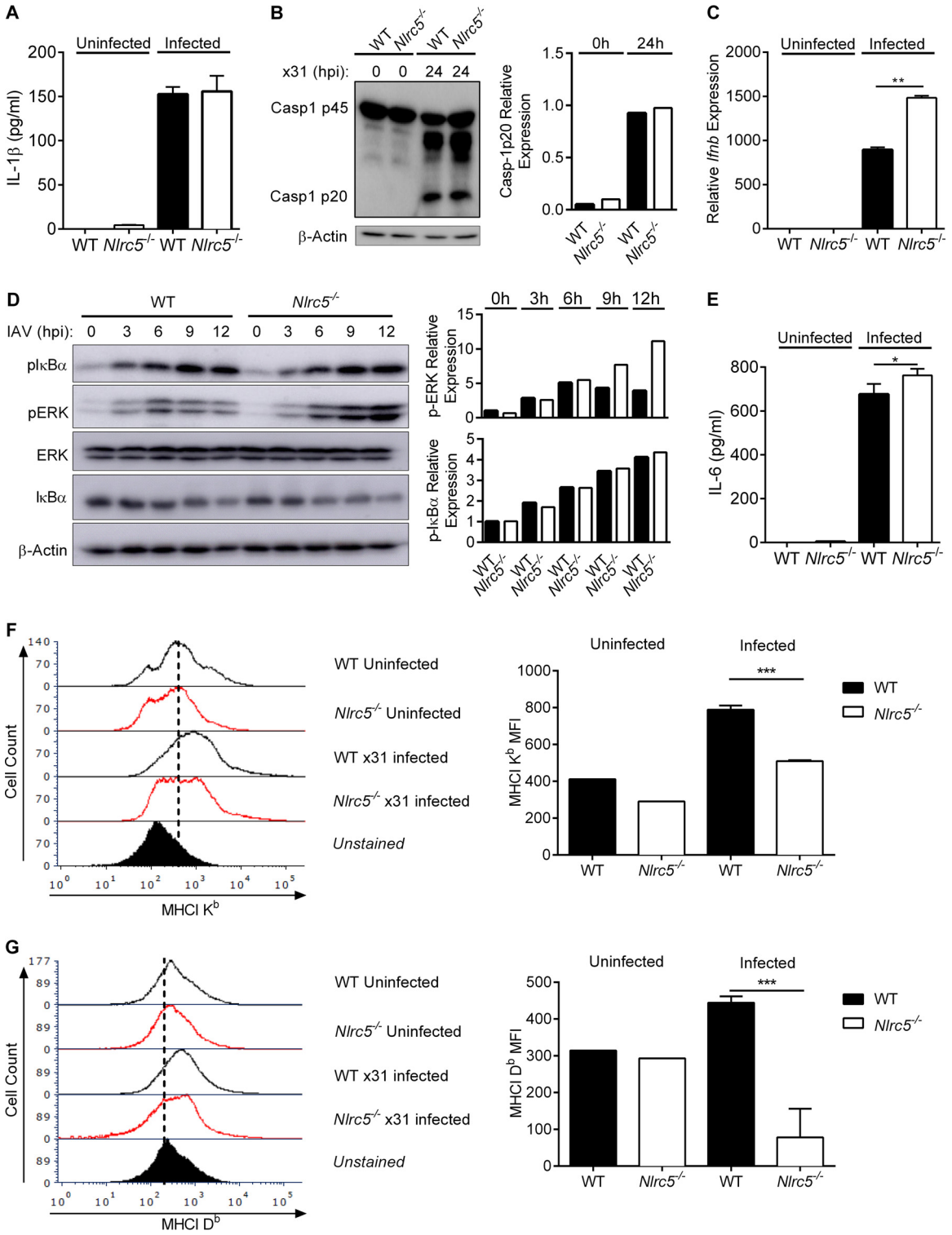

FIG 2 NLRC5 control of immune pathways during x31 infection *in vitro*. BMDCs from WT and *Nlrc5*$^{-/-}$ mice were mock infected or infected at an MOI of 10 with influenza A/HKx31 H3N2 (x31) virus for 24 h. (A) IL-1β levels in culture supernatants of uninfected and x31-infected BMDCs. (B) Western blotting of WT and *Nlrc5*$^{-/-}$ BMDC lysates for pro-caspase-1 (p45) and active caspase-1 (p20). (C) Expression levels of IFN-β (*Ifnb*) relative to those of β-actin in uninfected and x31-infected BMDCs. (D) WT and *Nlrc5*$^{-/-}$ BMDC lysates collected at the indicated time points were analyzed by Western blotting for phosphorylated and total ERK MAP kinase and IκBα as well as a GAPDH loading control. (E) IL-6 levels in the culture supernatants of uninfected or x31-infected BMDCs. (F and G) MHC-I K^b and D^b isoform expression levels were measured by flow cytometry and presented as geometric MFI. Data are representative of two independent experiments ($n = 2$ or 3 wells per experiment) and are means ± SEM. *, $P < 0.05$; **, $P < 0.01$; ***, $P < 0.001$ (two-sided unpaired Student's *t* test).

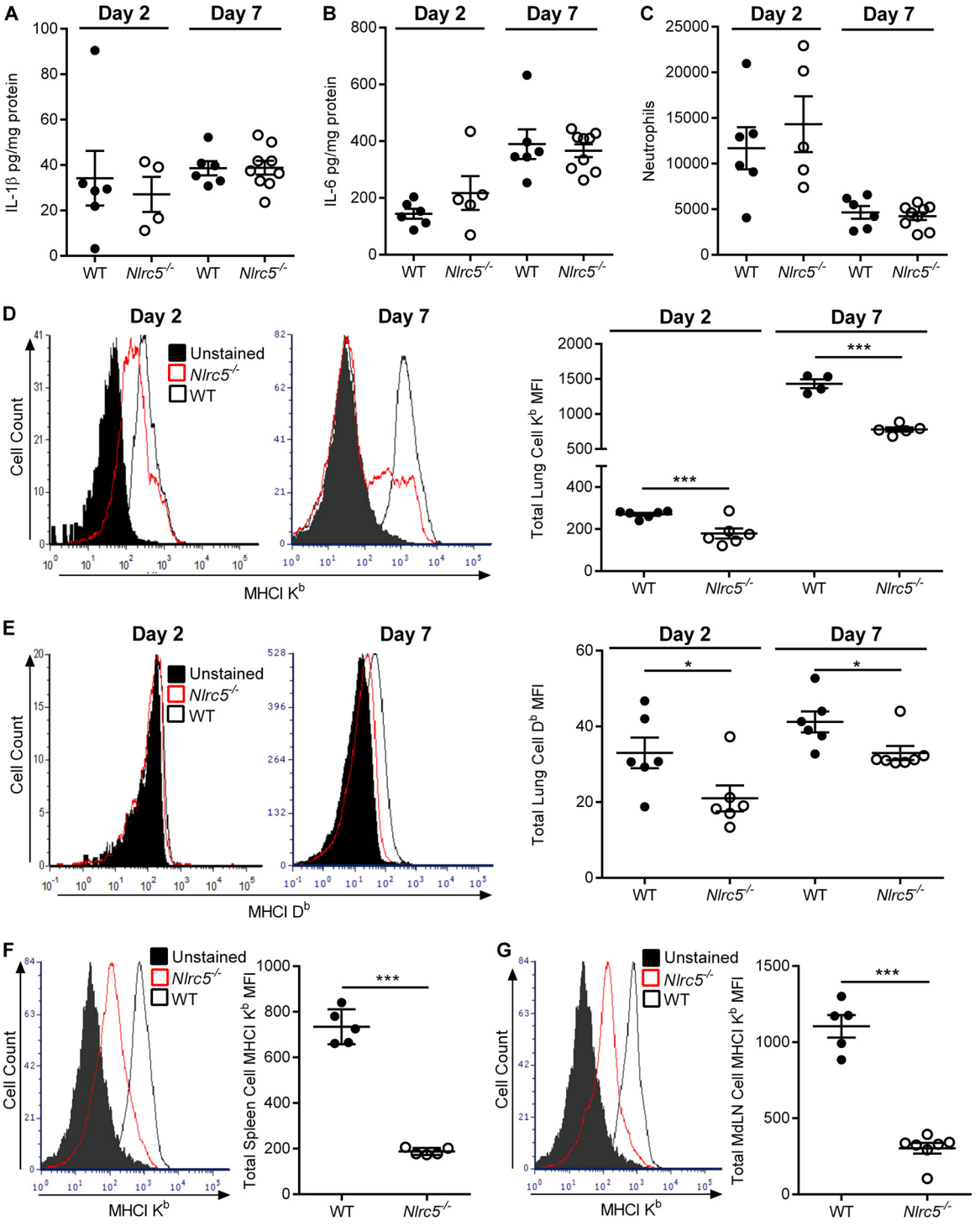

FIG 3 Effects of *Nlrc5* deletion in the lungs of IAV-infected mice. Mice were infected with 900 PFU of PR8 virus, and lungs were harvested on day 2 or 7 after infection. (A and B) Lung cytokine levels were determined on the indicated days after infection by ELISAs for IL-1β and IL-6. (C) Lung neutrophil numbers were determined by flow cytometry. (D to G) Flow cytometry examinations of MHC-I expression on total lung leukocytes (D and E), total spleen leukocytes (F), and total mediastinal lymph node (MdLN) leukocytes (G). The data are presented as geometric MFI. Data are representative of three or four independent experiments (n = 4 to 9 mice per genotype per experiment) and are means ± SEM. *, $P < 0.05$; ***, $P < 0.001$ (two-sided unpaired Student's t test).

those from WT controls on both days 2 and 7 after infection (Fig. 3D and E). Furthermore, this reduction in MHC-I levels was not confined to the site of infection, as MHC-I levels were lower on lymphocytes in the spleen (Fig. 3F) and lymphocytes in the mediastinal lymph nodes (MdLN) (Fig. 3G).

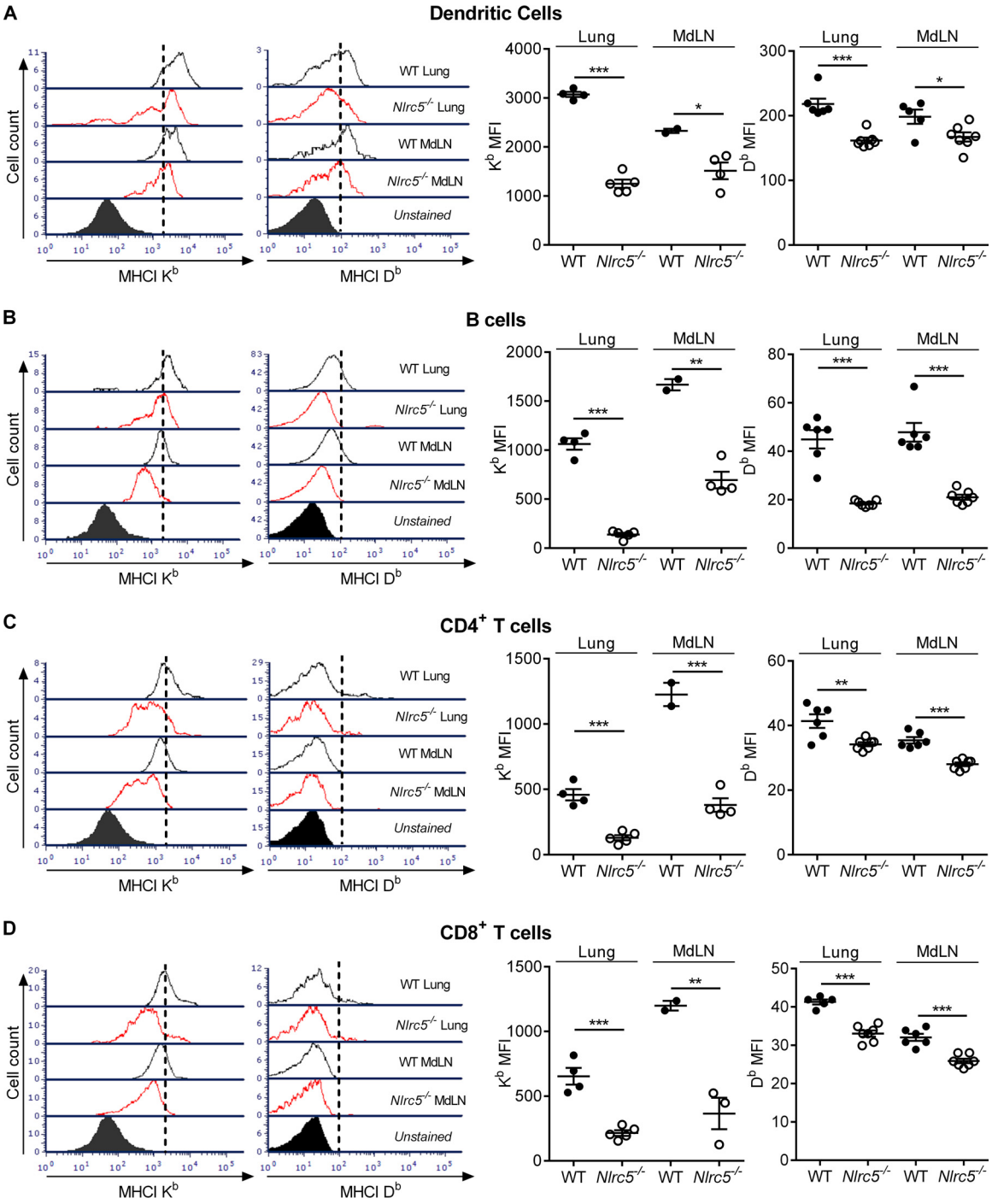

FIG 4 Effects of *Nlrc5* deletion on MHC-I expression in specific cell populations. Mice were infected with 900 PFU of PR8, and lungs were harvested on day 7 after infection. (A to D) Flow cytometry analyses of MHC-I expression in the indicated cell populations from the lungs and MdLN. Data are presented as geometric MFI. The data are representative of three or four independent experiments ($n = 4$ to 7 mice per genotype per experiment) and are means ± SEM. *, $P < 0.05$; **, $P < 0.01$; ***, $P < 0.001$ (two-sided unpaired Student's *t* test).

We further characterized the function of NLRC5 *in vivo* by examining MHC-I expression on various cell types. Expression levels of both MHC-I H2-D^b and H2-K^b were lower on dendritic cells (DCs) (Fig. 4A), B cells (Fig. 4B), CD4$^+$ T cells (Fig. 4C), and CD8$^+$ T cells (Fig. 4D) in the lungs and MdLN of *Nlrc5*$^{-/-}$ mice. These *in vivo* data demonstrate that deletion of *Nlrc5* decreases MHC-I expression on virtually all lymphocytes but does not affect expression of inflammasome- or NF-κB-dependent cytokines, such as IL-1β or IL-6, during PR8 infection.

Effects of diminished MHC-I expression on adaptive immune responses. MHC-I is essential for the generation and effector functions of $CD8^+$ T cells (22). Previous reports indicated that *Nlrc5*$^{-/-}$ mice have intrinsic defects in MHC-I expression and T cell numbers (10, 16). Indeed, we found that expression levels of MHC-I molecules on splenocytes were lower in naive *Nlrc5*$^{-/-}$ mice than in WT mice (Fig. 5A to D). $CD8^+$ T cell numbers were also lower in the spleens of *Nlrc5*$^{-/-}$ mice prior to infection with IAV, but $CD4^+$ T cell numbers were similar to those of WT controls (Fig. 5E and F). Therefore, we sought to determine the effects of *Nlrc5* deficiency and lower MHC-I expression on $CD8^+$ T cell responses during PR8 infection. To investigate whether NLRC5 deficiency leads to altered proliferation of $CD8^+$ T cells, we isolated T cells from the spleens of WT and *Nlrc5*$^{-/-}$ mice, labeled them with carboxyfluorescein succinimidyl ester (CFSE), and stimulated them *in vitro* with anti-CD3ε and anti-CD28 antibodies. We assessed T cell proliferation by CFSE dilution and found normal proliferation of *Nlrc5*$^{-/-}$ $CD8^+$ T cells (Fig. 5G).

Consistent with the observations for naive mice, total numbers of $CD8^+$ T cells were reduced in both the lungs and MdLN of *Nlrc5*$^{-/-}$ mice infected with PR8 on day 7 after infection (Fig. 6A and B). However, the number of IAV-specific $CD8^+$ T cells as determined by tetramer staining was not diminished for *Nlrc5*$^{-/-}$ mice compared to that for WT mice. Interestingly, we observed a shift in tetramer-specific populations between WT and *Nlrc5*$^{-/-}$ mice, with an increase in PB1-specific cells and a decrease in PA-specific cells in *Nlrc5*$^{-/-}$ mice (Fig. 6C and D). We also examined the functionality of the T cells and found a significant decrease in IFN-γ^+ $CD8^+$ T cells in *Nlrc5*$^{-/-}$ mice compared to those in WT mice (Fig. 6E). In addition, cytotoxic T cells from *Nlrc5*$^{-/-}$ mice had less expression of granzyme B (Fig. 6F). To validate the significance of these impaired effector responses on day 7 after infection, we injected PR8-infected mice with splenocytes that were pulsed with CD8-specific IAV peptides and labeled with CFSE. Mice were also injected with unpulsed splenocytes as a control. Examination of the ratio of pulsed to unpulsed cells after 12 h demonstrated that WT $CD8^+$ T cells were able to eliminate nearly all IAV peptide-pulsed cells, whereas *Nlrc5*$^{-/-}$ mice had significantly more IAV peptide-pulsed cells remaining (Fig. 6G). Because the peptides used to pulse these splenocytes were $CD8^+$ T cell specific, our results demonstrate a distinct functional defect in this cell population in *Nlrc5*$^{-/-}$ mice. Although $CD8^+$ T cell function was impaired, we did not observe any effect of *Nlrc5* deficiency on the total number of $CD4^+$ T cells or IFN-γ^+ $CD4^+$ T cells (Fig. 6H and I).

Altered immune responses affect virus clearance in *Nlrc5*$^{-/-}$ mice. To investigate whether NLRC5 deficiency alters virus replication and clearance, we assessed lung virus titers on days 2, 7, and 10 after PR8 infection (Fig. 7A to C). In line with defective $CD8^+$ T cell responses, higher viral loads were seen in the lungs of *Nlrc5*$^{-/-}$ mice on days 7 and 10 after infection (Fig. 7B and C). Virus titers were also higher at day 2, suggesting that innate immune responses were also impaired in *Nlrc5*$^{-/-}$ mice (Fig. 7A). Because of the altered immune response and increased virus titers, we examined whether *Nlrc5*$^{-/-}$ mice displayed enhanced morbidity or mortality. Surprisingly, *Nlrc5*$^{-/-}$ mice did not exhibit any difference in weight loss or mortality compared to that of WT mice in response to PR8 infection (Fig. 7D and E), and the only pathological difference in lungs was an increase in bronchial epithelial proliferation in *Nlrc5*$^{-/-}$ mice over that in WT mice (Fig. 7F).

Compensatory immune responses in *Nlrc5*-deficient mice during *in vivo* IAV infection. Despite significantly impaired $CD8^+$ T cell responses (Fig. 5E to G), only minor differences in virus titers and no noticeable differences in morbidity and mortality were observed for *Nlrc5*$^{-/-}$ mice. This prompted us to examine whether other immune mechanisms mitigate these outcomes in *Nlrc5*$^{-/-}$ mice. Humoral immunity is an important aspect of the adaptive immune response to IAV (23). We found that B cell numbers in the MdLN and IAV-specific antibody responses on days 7 and 12 after infection were normal in *Nlrc5*$^{-/-}$ mice (Fig. 8A to C). Because NLRC5 is implicated in regulating type I interferon production (14, 15), we examined this and found elevated

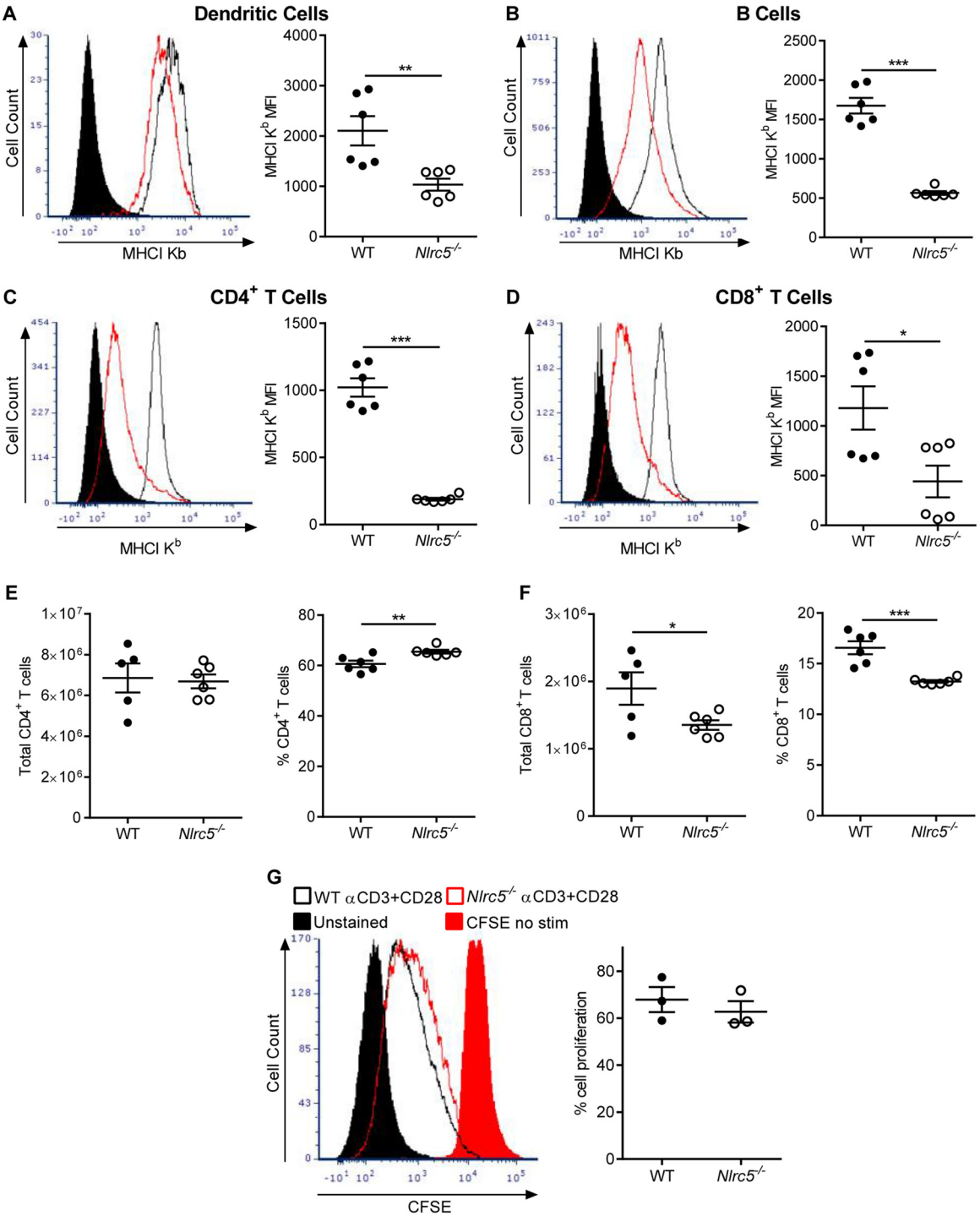

FIG 5 Naive *Nlrc5*$^{-/-}$ mice have intrinsic defects in MHC-I expression and CD8$^+$ T cell populations. (A to F) Spleens of naive mice were examined for MHC-I expression and T cell numbers by flow cytometry. (G) T cells isolated from the spleens of naive mice were labeled with CFSE and stimulated as indicated, or left unstimulated as a control. After 5 days, cells were analyzed by flow cytometry, and CFSE dilution was assessed as a measure of proliferation. In panels A to D, the data are presented as geometric MFI. The data are representative of two independent experiments ($n = 3$ mice per genotype per experiment) and are means ± SEM. *, $P < 0.05$; **, $P < 0.01$; ***, $P < 0.001$ (two-sided unpaired Student's *t* test).

IFN-β expression in the lungs of *Nlrc5*$^{-/-}$ mice (Fig. 8D). NK cells, which are innate lymphoid cells that are inhibited by MHC-I, might be more prevalent or more activated in *Nlrc5*$^{-/-}$ mice (24). Although their numbers were lower in the spleen prior to infection with IAV (Fig. 8E and F), NK cells were more prevalent in the lungs of *Nlrc5*$^{-/-}$

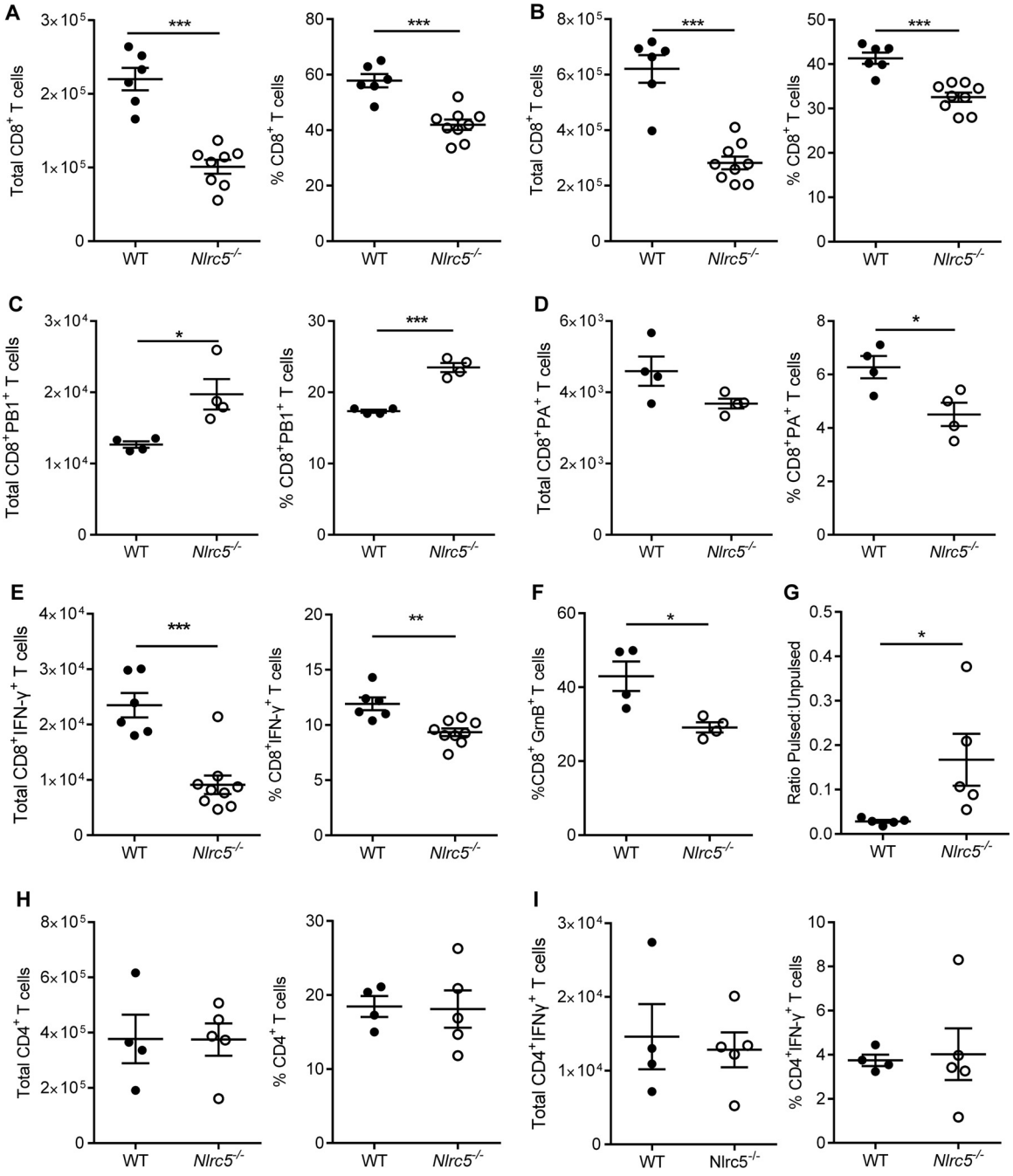

FIG 6 NLRC5 modulates the CD8$^+$ T cell response to IAV infection. Mice were infected with 900 PFU of PR8, and lungs and MdLN were harvested on day 7 after infection. Cells isolated from whole lungs and MdLN were examined for T cell responses. (A and B) Total lung (A) and MdLN (B) CD8$^+$ T cell numbers and percentages. (C and D) IAV tetramer-specific CD8$^+$ T cell numbers and percentages in the lungs. (E and F) Numbers and percentages of IFN-γ^+ or granzyme B$^+$ (GrnB$^+$) CD8$^+$ T cells in the lungs following *in vitro* restimulation. (G) *In vivo* cytotoxicity assay examining the ability of CD8$^+$ T cells to kill splenocytes pulsed with IAV-specific peptides versus unpulsed control splenocytes. (H and I) Total lung numbers and percentages of CD4$^+$ T cells (H) and IFN-γ^+ CD4$^+$ T cells (I) following *in vitro* restimulation. Data are representative of two to four independent experiments ($n = 4$ to 8 mice per genotype per experiment) and are means ± SEM. *, $P < 0.05$; **, $P < 0.01$; ***, $P < 0.001$ (two-sided unpaired Student's *t* test).

mice on day 7 after infection, and those cells tended to have increased granzyme B expression (not statistically significant) compared to that of WT controls (Fig. 8G to I). Together, these results suggest that multiple antiviral immune mechanisms are intact or enhanced in *Nlrc5*$^{-/-}$ mice during IAV infection and may compensate, to some extent, for the diminished CD8$^+$ T cell responses.

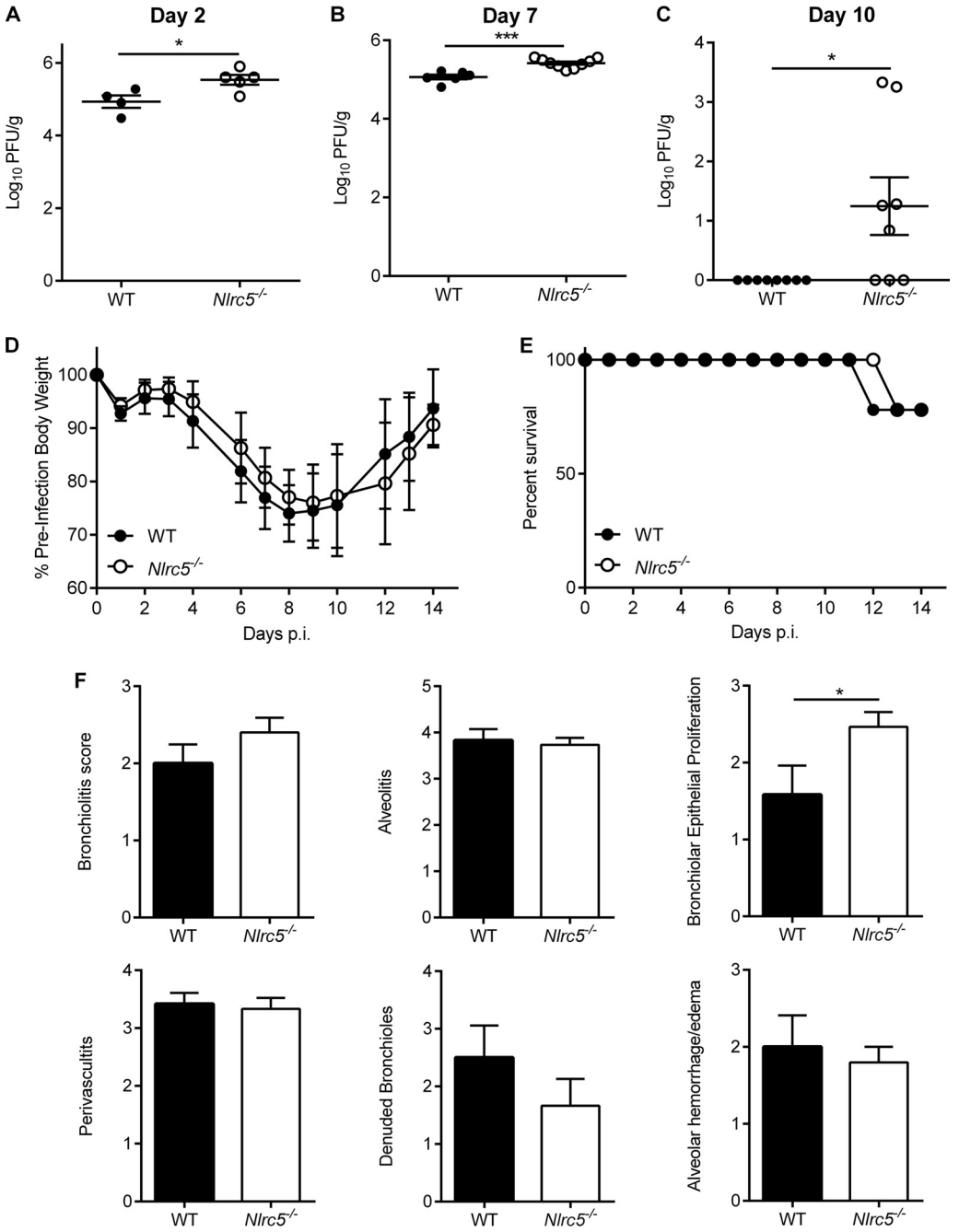

FIG 7 Effects of genetic deletion of NLRC5 on morbidity, mortality, and virus titer during IAV infection. Mice were infected with 900 PFU of PR8. (A to C) Lung viral loads were determined from whole-lung homogenates on days 2, 7, and 10 after infection. The weight loss (D) and mortality (E) of IAV-infected WT and *Nlrc5*$^{-/-}$ mice are shown. (F) Pathology analysis was performed for the indicated parameters on H&E-stained lung sections collected 7 days after PR8 infection. The data are representative of two to four independent experiments ($n = 4$ to 10 mice per genotype per experiment) and are means ± SEM. *, $P < 0.05$; ***, $P < 0.001$ (two-sided unpaired Student's *t* test for panels A and B; Mann-Whitney test for panel C).

DISCUSSION

Previous studies have reported diverse roles for NLRC5 in MHC-I expression, inflammasome activation, type I IFN responses, and the regulation of NF-κB signaling (12–21). Our results show that NLRC5 also plays an important role in MHC-I expression in the lungs, spleen, and MdLN both before and during IAV infection *in vivo*. MHC-I expression was decreased in CD4$^+$ and CD8$^+$ T cells, B cells, and dendritic cells from NLRC5-deficient mice. These data further confirm a key role for NLRC5 in regulation of MHC-I

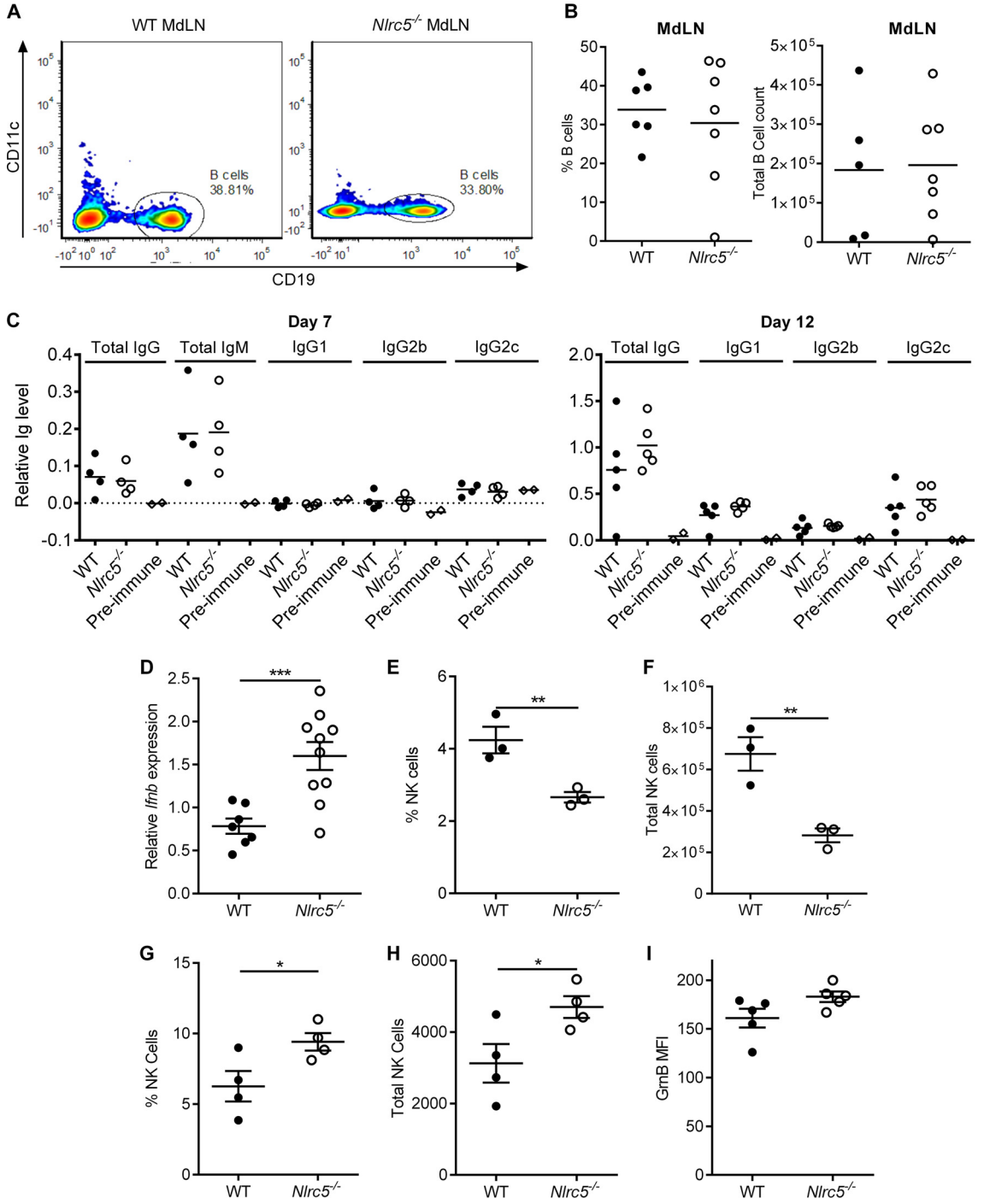

FIG 8 *Nlrc5*$^{-/-}$ mice have normal humoral and increased innate responses during IAV infection. Mice were infected with 900 PFU of PR8, and the spleen, lungs, serum, and MdLN were collected on the indicated days after infection. (A and B) Percentages and total numbers of B cells in the MdLN on day 7 after infection. (C) ELISA for PR8-specific serum antibody titers on days 7 and 12 after infection. Data are presented as relative antibody levels (OD_{450}). Preimmune mouse serum values show the baseline value for each isotype. (D) Lung IFN-β gene expression relative to that of β-actin on day 7 after infection. (E and F) Percentages and total numbers of spleen NK cells on day 0 (naive mice). (G and H) Percentages and total numbers of lung NK cells on day 7 after infection. (I) Expression of granzyme B (GrnB) in the NK cell population on day 7 after infection, as determined by flow cytometry. GrnB expression is presented as geometric MFI. All data are representative of two independent experiments ($n = 3$ to 5 mice per genotype per experiment) and are means ± SEM. *, $P < 0.05$; **, $P < 0.01$; ***, $P < 0.001$ (two-sided unpaired Student's t test).

expression. However, our data failed to demonstrate a role for NLRC5 in inflammasome activation in response to IAV infection. Furthermore, a significant effect of NLRC5 on NF-κB activation or IL-6 production was observed only during IAV infection *in vitro*. It should also be noted that IFN-β expression was elevated in *Nlrc5*$^{-/-}$ BMDCs *in vitro*,

especially with infection by the x31 virus. Although IFN-β expression was higher in *Nlrc5*$^{-/-}$ mice *in vivo*, virus titers were also higher at the same time points. Therefore, it remains to be tested whether NLRC5 directly regulates IFN-β expression during IAV infection or if a higher IFN-β level is merely a response to an increased virus load due to defects in other immune pathways.

Studies by Biswas et al. and Yao et al. reported that NLRC5 regulates MHC-I expression and cytotoxic CD8$^+$ T cell responses to *L. monocytogenes* infection (10, 16). These studies also showed reduced MHC-I expression on a variety of cells prior to stimulation. Stimulation of *Nlrc5*$^{-/-}$ cells with IFN-γ or lipopolysaccharide (LPS) or infection with *L. monocytogenes* failed to induce MHC-I expression to the same extent as that in WT cells (10, 16). Although *Nlrc5*$^{-/-}$ mice were found to have normal CD8$^+$ T cell development in the thymus, the numbers of CD8$^+$ T cells in the spleens of *Nlrc5*$^{-/-}$ mice were lower prior to infection (16). Yao et al. also showed a reduction in the relative proportion of CD8$^+$ T cells in the spleen following infection with *L. monocytogenes*. Both Biswas et al. and Yao et al. showed that CD8$^+$ T cells from *Nlrc5*$^{-/-}$ mice were functionally inferior in their cytotoxic activity, resulting in increased bacterial burdens in the spleen and liver (10, 16). Although Yao et al. reported minor differences in the production of IL-1β, neither group observed differences in type I IFN or IL-6 levels (16). In another model, Tong et al. demonstrated NLRC5 regulation of MHC-I expression during infection with vesicular stomatitis virus (VSV). However, NLRC5 only transiently regulated IL-6 and type I IFN, for the first 6 h following VSV infection (19). Another study, by Kumar and colleagues, reported no significant differences in the levels of IL-1β, IL-6, or other cytokines in *Nlrc5*$^{-/-}$ mice injected with the double-stranded RNA (dsRNA) analogue poly(I·C) (17). That study did not examine the effects of the *Nlrc5*$^{-/-}$ genotype on MHC-I expression. Based on the studies discussed above and our own data, it is clear that NLRC5 is important for the basal expression of MHC-I molecules and that the defect observed in its absence persists during infection. These data also demonstrate that *Nlrc5*$^{-/-}$ mice have intrinsic defects in peripheral CD8$^+$ T cell numbers and impaired CD8$^+$ T cell function during infection.

MHC-I presentation is important for activation of CD8$^+$ T cells (22). In our hands, this was associated with lower CD8$^+$ T cell numbers prior to infection and fewer IFN-γ- and granzyme B-producing CD8$^+$ T cells during IAV infection in *Nlrc5*$^{-/-}$ mice. Furthermore, IAV-specific CD8$^+$ T cells in *Nlrc5*$^{-/-}$ mice were less efficient at killing IAV peptide-pulsed cells in our *in vivo* experiments. The development of a Th1-biased, cytotoxic, pathogen-specific CD8$^+$ T cell response during IAV infection is important for resolving the infection (25, 26), and a slight defect in viral clearance was observed in our study, in association with diminished CD8$^+$ T cell responses in *Nlrc5*$^{-/-}$ mice. However, we did not observe any difference in weight loss or mortality during IAV infections of *Nlrc5*$^{-/-}$ mice and WT mice. Mice deficient in other molecules in the MHC-I expression pathway also exhibit a similar phenotype. Mice deficient in MHC-I H2-K^b and H2-D^b molecules (*K*^{b}*D*$^{b-/-}$) exhibit reduced numbers of CD8$^+$ T cells, but when challenged *in vivo*, they still generate CD8$^+$ MHC-I-specific allogeneic responses. Despite the lack of MHC-I K^b and D^b molecules, a minor population of functionally competent CD8$^+$ T cells arises in *K*^{b}*D*$^{b-/-}$ mice (27). It is also noteworthy that T cells are able to recognize target cells even with a very low MHC-I density (28). Antigen presentation in *Nlrc5*$^{-/-}$ cells has also been examined in other models. With DCs loaded with exogenous SIINFEKL peptide, *Nlrc5*-deficient DCs or B cells were able to activate and induce the proliferation of OT-I CD8$^+$ T cells despite reduced MHC-I expression (11, 29). However, when the SIINFEKL peptide was expressed endogenously by transfection of SIINFEKL mRNA within the *Nlrc5*$^{-/-}$ DCs, they displayed a slight reduction in antigen-presenting capacity compared to that of WT controls (29). Biswas et al. and Yao et al. also examined the ability of B cells or DCs to present SIINFEKL to CD8$^+$ T cells, and they found more prominent defects in CD8$^+$ T cell responses (10, 16). Although the reason for the observed differences in magnitude of the antigen-presenting defects is not clear, all these studies agree that, under some conditions, antigen-presenting cells from *Nlrc5*$^{-/-}$ mice have impaired antigen-presenting capacity. A study by Staehli et al. observed defective

killing of *Nlrc5*-deficient SIINFEKL peptide-pulsed target cells by OT-I T cells (11). This finding suggests that impaired pathogen clearance might be due to impaired target cell killing rather than a reduction in $CD8^+$ T cell numbers. This report is in line with our own data from IAV-infected mice. *In vivo*, we observed only a shift in the $CD8^+$ T cell epitope dominance, with increased PB1-specific cells and decreased PA-specific cells. However, the functionality of these IAV-specific cells was compromised in *Nlrc5*$^{-/-}$ mice. Overall, our data and the previous reports discussed above support a role for NLRC5 in determining the robustness of MHC-I–$CD8^+$ T cell interactions. However, the observed reduction in MHC-I results in only a minor defect in antigen-specific $CD8^+$ T cell functionality, but not T cell proliferation, in our model.

Other than $CD8^+$ T cells, humoral immune responses as well as innate immune responses are important during IAV infection. The intact humoral immune responses in *Nlrc5*$^{-/-}$ mice may prevent the development of severe disease in our model, in which only modestly impaired cellular immunity was observed (23). Although it is not clear whether the increase in IFN-β observed in *Nlrc5*$^{-/-}$ mice is a consequence of higher virus titers or is specific to *Nlrc5* deletion, higher IFN-β levels may also be beneficial to the host in cases of impaired cellular immunity. In addition to these, NK cells may further constitute a compensatory mechanism in *Nlrc5*$^{-/-}$ mice infected with IAV. NK cells play an important role in the early antiviral immune response by killing infected cells and regulating later adaptive immunity (30). During IAV infection, the NK cell-activating receptor NKp46 can interact with IAV hemagglutinin (HA) to kill infected cells (31). The murine receptor corresponding to NKp46, NCR1, has also been shown to affect the immune response to IAV (32). Multiple clinical studies have reported a decrease or absence of circulating NK cells in IAV-infected patients with severe symptoms (33–35). Although NK cell numbers were lower prior to infection in our mice, we observed increased NK cell numbers in the lungs of *Nlrc5*$^{-/-}$ mice on day 7 after IAV infection. Thus, NK cell responses may act to counterbalance the defective $CD8^+$ T cell responses observed in *Nlrc5*$^{-/-}$ mice. Notably, Ludigs et al. recently showed that T cell-specific deletion of *Nlrc5* enhanced NK cell cytotoxicity (24). Therefore, *Nlrc5*$^{-/-}$ mice may prove to be an interesting tool for studying compensatory mechanisms in the immune response and warrant future studies to investigate these responses during IAV infection.

Overall, our study demonstrates that the NLR family member NLRC5 is important for MHC-I expression in naive mice and the effector $CD8^+$ T cell functions in response to IAV infection. Our data also indicate that impaired cytotoxic T cell responses in *Nlrc5*$^{-/-}$ mice might be compensated through increased NK cell and type I IFN responses and normal humoral immunity. These findings add to our knowledge of the functional diversity of innate immune sensors and the induction of host protective responses during viral infection and may aid in the development of therapies or vaccines that can alter T cell epitope dominance or enhance $CD8^+$ T cell or NK cell responses to combat infection.

MATERIALS AND METHODS

Mice. *Nlrc5*$^{-/-}$ mice on the C57BL/6J background have been reported previously (10, 16, 17). WT C57BL/6J mice were purchased from Jackson Laboratory and subsequently bred in-house at St. Jude Children's Research Hospital (SJCRH) for more than 5 generations, in the same animal room as that for *Nlrc5*$^{-/-}$ mice, prior to beginning experiments. For experiments with the x31 virus, WT and *Nlrc5*$^{-/-}$ mice were cohoused in the same cage for 2 weeks prior to harvest of bone marrow. All mice were bred and maintained at SJCRH. All animal experiments were conducted under protocols approved by the St. Jude Children's Research Hospital Committee on Use and Care of Animals (protocol 482) and were performed in accordance with institutional policies, AAALAC guidelines, the American Veterinary Medical Association (AVMA) guidelines on euthanasia, NIH regulations (36), and the U.S. Animal Welfare Act of 1966.

Viruses. The influenza A/Puerto Rico/8/34 H1N1 virus (PR8) and the influenza A/HKx31 H3N2 virus (x31) were generated using an eight-plasmid reverse genetics system (37). Stocks were propagated up to two times by allantoic inoculation of 10-day-old embryonated chicken eggs with seed virus diluted 10^{-4}. The stock virus concentration was determined by the plaque assay method as previously reported (38). Dendritic cells were infected at a multiplicity of infection (MOI) of 10 with either virus. Influenza A/Puerto Rico/8/34 H1N1 virus (PR8) was used for all *in vivo* experiments.

***In vivo* infection.** Mice were anesthetized with 5 mg tribromoethanol (Avertin) administered via intraperitoneal injection and then infected with PR8 virus at a dose of 900 PFU administered intranasally in 30 μl of phosphate-buffered saline. Mice were monitored until they recovered from anesthesia. For all experiments, animals infected with IAV were weighed and monitored daily for signs of distress. Mice were euthanized by CO_2 asphyxiation followed by cervical dislocation at the indicated times after infection (day 0, 2, 7, 10, or 12 postinfection [p.i.]). For survival experiments, animals were euthanized by CO_2 asphyxiation followed by cervical dislocation when they lost 33% of their preinfection weight or became moribund.

***In vitro* BMDC stimulation.** WT and *Nlrc5*$^{-/-}$ BMDCs were differentiated as previously described, using granulocyte-macrophage colony-stimulating factor (GM-CSF) (38). Day 7 BMDCs were infected with IAV at an MOI of 10, and samples were collected for flow cytometry at 24 h p.i. Samples were also tested for cytokine levels by enzyme-linked immunosorbent assay (ELISA) or quantitative real-time PCR (qRT-PCR). For flow cytometry, cells were stained with anti-CD80, -CD11c, -MHC-I H2-K^b, and -MHC-I H2-D^b (16-10A11, N418, AF6-88.5, and KH95; Biolegend, San Diego, CA). Data were analyzed using FlowJo (FlowJo, LLC, Ashland, OR), and the geometric mean fluorescence intensity (MFI) was calculated using FlowJo.

Quantification of lung viral loads. Lungs were harvested from WT and *Nlrc5*$^{-/-}$ mice infected i.n. with 900 PFU of IAV on the indicated day after infection. Lung viral titers were determined as previously reported (38). Briefly, diluted lung homogenates were plated on Madin-Darby canine kidney (MDCK) cells. After a period of infection, the cells were washed and overlaid with minimum essential medium (MEM) containing agarose (Lonza, Basel, Switzerland). After 3 days, agar plugs were removed, and plaques were visualized using crystal violet.

Flow cytometric analysis of lung, spleen, and mediastinal lymph node cells. Mice were infected i.n. with 900 PFU of IAV. Mice were euthanized on day 0, 2, 7, 10, or 12 for sampling of the whole lungs, spleen, mediastinal lymph nodes (MdLN), or blood serum. Cells from the lungs were isolated following red blood cell (RBC) lysis, using a Percoll gradient. Spleen and MdLN cells were isolated directly after RBC lysis. Dendritic cells were identified by staining with anti-CD86 and -CD11c antibodies (GL-1 and N-418; Biolegend) and anti-MHC-II antibody (MHCII, MS/114.15.2; eBioscience, San Diego, CA). Neutrophils were gated as Gr-1$^+$ and CD11b$^+$ cells (RB6-8C5 and M1/70; Biolegend). B cells were identified using a CD19$^+$ (6D5; Biolegend) gating strategy. T cell responses were examined by flow cytometry after staining with anti-T cell receptor β (anti-TCR-β), anti-CD8, and anti-CD4 antibodies (H57-597, 53-6.7, and RM4-5; Biolegend). NK cells were stained and gated as NK1.1$^+$ CD3$^-$ cells (PK136 and 17A2; Biolegend). For intracellular cytokine staining, we stained lung samples with anti-granzyme B (GB11; BD Biosciences), anti-gamma interferon (XMG1.2; Biolegend), or anti-tumor necrosis factor alpha (anti-TNF-α) (MP6-XT22; Biolegend) after stimulation with a cocktail of IAV peptides ($PB1_{703–711}$, $PB1\text{-}F2_{62–70}$, $NP_{366–374}$, $PA_{224–233}$, and $NS2_{114–121}$) in the presence of monensin for CD8$^+$ T cells or phorbol myristate acetate (PMA)-ionomycin-monensin for CD4$^+$ T cells. Cells were analyzed using an LSR II flow cytometer (BD Biosciences, San Jose, CA). Data were analyzed in FlowJo (FlowJo, LLC). Total cell numbers were calculated by multiplying the percentage of positive cells acquired by the total number of cells isolated.

***In vitro* T cell proliferation.** We examined the proliferation of CD8$^+$ T cells *in vitro* by CFSE staining. T cells were isolated from mouse spleens and labeled with 1.5 μg/ml of CFSE (eBioscience). Cells were then plated in RP10 medium in the presence or absence of plate-bound anti-CD3ε and -CD28 antibodies (145-2C11 and 37.51; eBioscience) for 3 days, followed by IL-2 (10 μg/ml) for 2 days. Cells were then stained with anti-CD8 and -CD4 antibodies and examined by flow cytometry for CFSE dilution.

***In vivo* cytotoxicity.** To examine the *in vivo* cytotoxic capacity of CD8$^+$ T cells, WT splenocytes were labeled with a high concentration of CFSE (1.5 μg/ml) and pulsed with CD8-specific IAV peptides ($PB1_{703–711}$, $PB1\text{-}F2_{62–70}$, $NP_{366–374}$, $PA_{224–233}$, and $NS2_{114–121}$). Another set of WT splenocytes was stained with a low concentration of CFSE (0.15 μg/ml) but not pulsed with IAV peptides, as a control. Mice that had been infected with IAV for 7 days were then injected with a 1:1 mixture of the pulsed and unpulsed splenocytes. Spleens of IAV-infected mice were removed 12 h after injection, and the ratio of pulsed CFSE^{high} to unpulsed CFSE^{low} splenocytes was determined by flow cytometry.

Cytokine quantification. Cytokine levels in cell culture supernatants or whole-lung homogenates were analyzed using Ready-Set-Go IL-6 or IL-1β ELISA kits following the manufacturer's instructions (eBioscience). All cytokines from lung homogenates were normalized to the total protein in the homogenate by the bicinchoninic acid (BCA) protein assay (Pierce, Rockford, IL), and their concentrations were expressed as picograms of cytokine per milligram of total protein.

IAV-specific antibody ELISA. IAV was partially purified through a 30% sucrose cushion, and virions were lysed in RIPA buffer. Lysate was diluted in bicarbonate ELISA coating buffer and used to coat ELISA plates. Pre- and postinfection sera from mice were diluted and added to ELISA plates after blocking with 1× ELISA/ELISPOT assay buffer (eBioscience). Isotype-specific mouse anti-IAV antibodies were detected using a C57BL/6-HRP SBA clonotyping system (Southern Biotech). Relative antibody levels were measured by determining the optical density at 450 nm (OD_{450}) after tetramethylbenzidine (TMB) substrate addition and quenching with 1 N H_2SO_4.

qRT-PCR. Total RNA was isolated using the Trizol method (Life Technologies, Carlsbad, CA). First-strand cDNA was generated from total RNA by use of high-capacity cDNA reverse transcription reagents (Applied Biosystems, Foster City, CA). cDNA samples were prepared and subjected to qRT-PCR on an ABI Prism 7900 instrument, using SYBR green PCR master mix (Applied Biosystems), and the results were normalized to the β-actin housekeeping gene. The following primer pairs were used for qRT-PCR analysis: for mouse β-actin, 5′-GGCTGTATTCCCCTCCATCG-3′ (forward) and 5′-CCAGTTGGTAACAATGCCATGT-3′

(reverse); and for mouse IFN-β, 5′-GCCTTTGCCATCCAAGAGATGC-3′ (forward) and 5′-ACACTGTCTGCTG GTGGAGTTC-3′ (reverse). qRT-PCR data were determined according to the standard curve method.

Histopathology. The left lobes of the lungs from each mouse were formalin fixed, paraffin embedded, and processed by standard techniques at the Veterinary Pathology Core at SJCRH. Longitudinal 5-μm sections were stained with hematoxylin and eosin (H&E), and histopathological analysis was conducted by an experienced pathologist blinded to the experimental groups (Peter Vogel, SJCRH).

Statistical analysis. GraphPad Prism 6.0 software was used for data analysis. Data are presented as means ± standard errors of the means (SEM) or standard deviations (SD). Statistical significance was determined by Student's *t* test for single comparisons, two-way analysis of variance (ANOVA) for weight loss, and the Kaplan-Meyer test for survival studies. *P* values of <0.05 were considered statistically significant.

ACKNOWLEDGMENTS

We thank Shizuo Akira for generously supplying the *Nlrc5*$^{-/-}$ mice. We thank the flow cytometry core in the Department of Immunology at St. Jude Children's Research Hospital. We also thank Paul Thomas at St. Jude Children's Research Hospital for providing the x31 virus and IAV-specific peptides for CD8$^+$ T cell restimulation and Peter Vogel for histopathology analysis.

Research studies from our laboratory are supported by the U.S. National Institutes of Health (grants AI101935, AI124346, AR056296, and CA163507 to T.-D.K.) and the American Lebanese Syrian Associated Charities (to T.-D.K.).

We declare that we have no competing financial interests.

This research is the sole responsibility of the authors and does not necessarily reflect the views of the funding agencies.

REFERENCES

1. WHO. April 2009. Influenza (seasonal) fact sheet no. 211. WHO, Geneva, Switzerland. http://www.who.int/mediacentre/factsheets/fs211/en/index.html. Accessed 12 June 2012.
2. Thomas PG, Dash P, Aldridge JR, Jr, Ellebedy AH, Reynolds C, Funk AJ, Martin WJ, Lamkanfi M, Webby RJ, Boyd KL, Doherty PC, Kanneganti TD. 2009. The intracellular sensor NLRP3 mediates key innate and healing responses to influenza A virus via the regulation of caspase-1. Immunity 30:566–575. https://doi.org/10.1016/j.immuni.2009.02.006.
3. Allen IC, Scull MA, Moore CB, Holl EK, McElvania-TeKippe E, Taxman DJ, Guthrie EH, Pickles RJ, Ting JP. 2009. The NLRP3 inflammasome mediates in vivo innate immunity to influenza A virus through recognition of viral RNA. Immunity 30:556–565. https://doi.org/10.1016/j.immuni.2009.02.005.
4. Ichinohe T, Lee HK, Ogura Y, Flavell R, Iwasaki A. 2009. Inflammasome recognition of influenza virus is essential for adaptive immune responses. J Exp Med 206:79–87. https://doi.org/10.1084/jem.20081667.
5. Sabbah A, Chang TH, Harnack R, Frohlich V, Tominaga K, Dube PH, Xiang Y, Bose S. 2009. Activation of innate immune antiviral responses by Nod2. Nat Immunol 10:1073–1080. https://doi.org/10.1038/ni.1782.
6. Lupfer C, Thomas PG, Kanneganti TD. 2014. Nucleotide oligomerization and binding domain 2-dependent dendritic cell activation is necessary for innate immunity and optimal CD8$^+$ T cell responses to influenza A virus infection. J Virol 88:8946–8955. https://doi.org/10.1128/JVI.01110-14.
7. Beresford GW, Boss JM. 2001. CIITA coordinates multiple histone acetylation modifications at the HLA-DRA promoter. Nat Immunol 2:652–657. https://doi.org/10.1038/89810.
8. Meissner TB, Li A, Biswas A, Lee KH, Liu YJ, Bayir E, Iliopoulos D, van den Elsen PJ, Kobayashi KS. 2010. NLR family member NLRC5 is a transcriptional regulator of MHC class I genes. Proc Natl Acad Sci U S A 107:13794–13799. https://doi.org/10.1073/pnas.1008684107.
9. Robbins GR, Truax AD, Davis BK, Zhang L, Brickey WJ, Ting JP. 2012. Regulation of class I major histocompatibility complex (MHC) by nucleotide-binding domain, leucine-rich repeat-containing (NLR) proteins. J Biol Chem 287:24294–24303. https://doi.org/10.1074/jbc.M112.364604.
10. Biswas A, Meissner TB, Kawai T, Kobayashi KS. 2012. Cutting edge: impaired MHC class I expression in mice deficient for Nlrc5/class I transactivator. J Immunol 189:516–520. https://doi.org/10.4049/jimmunol.1200064.
11. Staehli F, Ludigs K, Heinz LX, Seguin-Estevez Q, Ferrero I, Braun M, Schroder K, Rebsamen M, Tardivel A, Mattmann C, MacDonald HR, Romero P, Reith W, Guarda G, Tschopp J. 2012. NLRC5 deficiency selectively impairs MHC class I-dependent lymphocyte killing by cytotoxic T cells. J Immunol 188:3820–3828. https://doi.org/10.4049/jimmunol.1102671.
12. Benko S, Magalhaes JG, Philpott DJ, Girardin SE. 2010. NLRC5 limits the activation of inflammatory pathways. J Immunol 185:1681–1691. https://doi.org/10.4049/jimmunol.0903900.
13. Cui J, Zhu L, Xia X, Wang HY, Legras X, Hong J, Ji J, Shen P, Zheng S, Chen ZJ, Wang RF. 2010. NLRC5 negatively regulates the NF-kappaB and type I interferon signaling pathways. Cell 141:483–496. https://doi.org/10.1016/j.cell.2010.03.040.
14. Neerincx A, Lautz K, Menning M, Kremmer E, Zigrino P, Hosel M, Buning H, Schwarzenbacher R, Kufer TA. 2010. A role for the human nucleotide-binding domain, leucine-rich repeat-containing family member NLRC5 in antiviral responses. J Biol Chem 285:26223–26232. https://doi.org/10.1074/jbc.M110.109736.
15. Ranjan P, Singh N, Kumar A, Neerincx A, Kremmer E, Cao W, Davis WG, Katz JM, Gangappa S, Lin R, Kufer TA, Sambhara S. 2015. NLRC5 interacts with RIG-I to induce a robust antiviral response against influenza virus infection. Eur J Immunol 45:758–772. https://doi.org/10.1002/eji.201344412.
16. Yao Y, Wang Y, Chen F, Huang Y, Zhu S, Leng Q, Wang H, Shi Y, Qian Y. 2012. NLRC5 regulates MHC class I antigen presentation in host defense against intracellular pathogens. Cell Res 22:836–847. https://doi.org/10.1038/cr.2012.56.
17. Kumar H, Pandey S, Zou J, Kumagai Y, Takahashi K, Akira S, Kawai T. 2011. NLRC5 deficiency does not influence cytokine induction by virus and bacteria infections. J Immunol 186:994–1000. https://doi.org/10.4049/jimmunol.1002094.
18. Kuenzel S, Till A, Winkler M, Hasler R, Lipinski S, Jung S, Grotzinger J, Fickenscher H, Schreiber S, Rosenstiel P. 2010. The nucleotide-binding oligomerization domain-like receptor NLRC5 is involved in IFN-dependent antiviral immune responses. J Immunol 184:1990–2000. https://doi.org/10.4049/jimmunol.0900557.
19. Tong Y, Cui J, Li Q, Zou J, Wang HY, Wang RF. 2012. Enhanced TLR-induced NF-kappaB signaling and type I interferon responses in NLRC5 deficient mice. Cell Res 22:822–835. https://doi.org/10.1038/cr.2012.53.
20. Davis BK, Roberts RA, Huang MT, Willingham SB, Conti BJ, Brickey WJ, Barker BR, Kwan M, Taxman DJ, Accavitti-Loper MA, Duncan JA, Ting JP. 2011. Cutting edge: NLRC5-dependent activation of the inflammasome. J Immunol 186:1333–1337. https://doi.org/10.4049/jimmunol.1003111.
21. Triantafilou K, Kar S, van Kuppeveld FJ, Triantafilou M. 2013. Rhinovirus-induced calcium flux triggers NLRP3 and NLRC5 activation in bronchial

cells. Am J Respir Cell Mol Biol 49:923–934. https://doi.org/10.1165/rcmb.2013-0032OC.
22. Zijlstra M, Bix M, Simister NE, Loring JM, Raulet DH, Jaenisch R. 1990. Beta 2-microglobulin deficient mice lack CD4−8+ cytolytic T cells. Nature 344:742–746. https://doi.org/10.1038/344742a0.
23. Mozdzanowska K, Furchner M, Zharikova D, Feng J, Gerhard W. 2005. Roles of CD4+ T-cell-independent and -dependent antibody responses in the control of influenza virus infection: evidence for noncognate CD4+ T-cell activities that enhance the therapeutic activity of antiviral antibodies. J Virol 79:5943–5951. https://doi.org/10.1128/JVI.79.10.5943-5951.2005.
24. Ludigs K, Jandus C, Utzschneider DT, Staehli F, Bessoles S, Dang AT, Rota G, Castro W, Zehn D, Vivier E, Held W, Romero P, Guarda G. 2016. NLRC5 shields T lymphocytes from NK-cell-mediated elimination under inflammatory conditions. Nat Commun 7:10554. https://doi.org/10.1038/ncomms10554.
25. Bender BS, Croghan T, Zhang L, Small PA, Jr. 1992. Transgenic mice lacking class I major histocompatibility complex-restricted T cells have delayed viral clearance and increased mortality after influenza virus challenge. J Exp Med 175:1143–1145. https://doi.org/10.1084/jem.175.4.1143.
26. Mackenzie CD, Taylor PM, Askonas BA. 1989. Rapid recovery of lung histology correlates with clearance of influenza virus by specific CD8+ cytotoxic T cells. Immunology 67:375–381.
27. Vugmeyster Y, Glas R, Perarnau B, Lemonnier FA, Eisen H, Ploegh H. 1998. Major histocompatibility complex (MHC) class I KbDb −/− deficient mice possess functional CD8+ T cells and natural killer cells. Proc Natl Acad Sci U S A 95:12492–12497. https://doi.org/10.1073/pnas.95.21.12492.
28. Sykulev Y, Joo M, Vturina I, Tsomides TJ, Eisen HN. 1996. Evidence that a single peptide-MHC complex on a target cell can elicit a cytolytic T cell response. Immunity 4:565–571. https://doi.org/10.1016/S1074-7613(00)80483-5.
29. Rota G, Ludigs K, Siegert S, Tardivel A, Morgado L, Reith W, De Gassart A, Guarda G. 2016. T cell priming by activated Nlrc5-deficient dendritic cells is unaffected despite partially reduced MHC class I levels. J Immunol 196:2939–2946. https://doi.org/10.4049/jimmunol.1502084.
30. Vivier E, Tomasello E, Baratin M, Walzer T, Ugolini S. 2008. Functions of natural killer cells. Nat Immunol 9:503–510. https://doi.org/10.1038/ni1582.
31. Mandelboim O, Lieberman N, Lev M, Paul L, Arnon TI, Bushkin Y, Davis DM, Strominger JL, Yewdell JW, Porgador A. 2001. Recognition of haemagglutinins on virus-infected cells by NKp46 activates lysis by human NK cells. Nature 409:1055–1060. https://doi.org/10.1038/35059110.
32. Gazit R, Gruda R, Elboim M, Arnon TI, Katz G, Achdout H, Hanna J, Qimron U, Landau G, Greenbaum E, Zakay-Rones Z, Porgador A, Mandelboim O. 2006. Lethal influenza infection in the absence of the natural killer cell receptor gene Ncr1. Nat Immunol 7:517–523.
33. Denney L, Aitken C, Li CK, Wilson-Davies E, Kok WL, Clelland C, Rooney K, Young D, Dong T, McMichael AJ, Carman WF, Ho LP. 2010. Reduction of natural killer but not effector CD8 T lymphocytes in three consecutive cases of severe/lethal H1N1/09 influenza A virus infection. PLoS One 5:e10675. https://doi.org/10.1371/journal.pone.0010675.
34. Guo X, Chen Y, Li X, Kong H, Yang S, Ye B, Cui D, Wu W, Li L. 2011. Dynamic variations in the peripheral blood lymphocyte subgroups of patients with 2009 pandemic H1N1 swine-origin influenza A virus infection. Virol J 8:215. https://doi.org/10.1186/1743-422X-8-215.
35. Jost S, Quillay H, Reardon J, Peterson E, Simmons RP, Parry BA, Bryant NN, Binder WD, Altfeld M. 2011. Changes in cytokine levels and NK cell activation associated with influenza. PLoS One 6:e25060. https://doi.org/10.1371/journal.pone.0025060.
36. National Research Council. 2011. Guide for the care and use of laboratory animals, 8th ed. National Academies Press, Washington, DC.
37. Hoffmann E, Krauss S, Perez D, Webby R, Webster RG. 2002. Eight-plasmid system for rapid generation of influenza virus vaccines. Vaccine 20:3165–3170. https://doi.org/10.1016/S0264-410X(02)00268-2.
38. Lupfer C, Thomas PG, Anand PK, Vogel P, Milasta S, Martinez J, Huang G, Green M, Kundu M, Chi H, Xavier RJ, Green DR, Lamkanfi M, Dinarello CA, Doherty PC, Kanneganti TD. 2013. Receptor interacting protein kinase 2-mediated mitophagy regulates inflammasome activation during virus infection. Nat Immunol 14:480–488. https://doi.org/10.1038/ni.2563.